

---

**COAXIAL GYRO-BWO. 2. THE NONLINEAR THEORY****A.V. BORODKIN, G.V. SOTNIKOV, I.N. ONISHCHENKO,  
V.M. KHORUZHIIY**UDC 621.372.8  
©2005**National Science Center "Kharkiv Institute of Physics and Technology"**  
(1, Akademichna Str., Kharkiv 61108, Ukraine; e-mail: khoruzhiy@kipt.kharkov.ua)

---

Theoretical and numerical investigations of a nonlinear regime of generation in a coaxial backward wave oscillator (gyro-BWO) operating at the resonance of an electron beam with the eigenmode of a coaxial waveguide on the normal Doppler effect are carried out. The spatio-temporal dependences of the HF wave amplitude in a coaxial waveguide for various values of injected electron beam currents are analyzed. Types of excitation regimes of a coaxial gyro-BWO and the behavior of the interaction efficiency when changing the electron beam current are investigated.

---

**1. Introduction**

A gyro-BWO is a high-power HF-generator acting in the range of cm- and mm-wavelengths, in which the interaction of an electron beam with a backward wave excited on the normal Doppler effect is used. Some of the advantages of a gyro-BWO (as those of other gyro-devices) are *a*) the relative simplicity of the construction (a section of the waveguide), *b*) a high value of the constant longitudinal magnetic field is simultaneously a focusing one for high-current electron beams, and *c*) a rather weak dependence on the initial longitudinal spread of the beam energy. The shortcoming is a relatively small efficiency which is a consequence of the longitudinal distribution of the excited electric HF field. In this case, the modulation of an injected beam occurs at a maximum of the HF-field, and the following generation takes place in the HF-field decreasing at the oscillator output up to zero. This longitudinal structure of the excited field is such that a regrouping of electrons happens.

The first investigations of nonlinear regimes of the generation of HF-oscillations in a gyro-BWO

were done in [1,2]. In [1], in particular, the steady-state conditions in a gyro-BWO depending on the initial transversal energy of a electron beam were considered. The longitudinal distributions of the HF-field amplitude along the generator presented in [1] have allowed one to classify the effects of the interaction occurring in a gyro-BWO. Investigations of the dependence of the electron efficiency on both the nonisochronism parameter and the system length have shown that the total efficiency does not exceed 10 % even for optimal fitted parameters. In [2], the self-consistent 3D theory of a gyro-BWO in a steady-state regime and the effect of the longitudinal dispersion of velocities in the beam on efficiency are presented. A dispersion up to 5 % changes the efficiency only slightly. Upon the further increase in the dispersion up to 10 %, the efficiency is decreased by two times. It is also shown in [2] that the efficiency can be increased by the creation of a weak inhomogeneity of the constant longitudinal magnetic field (the numerical calculations have shown that the efficiency is incremented by 8-23 % in comparison with the case of a homogeneous magnetic field).

The theoretical and experimental researches of coaxial gyro-BWOs are on the initial stage. In [3], a coaxial gyro-BWO in the linear regime was theoretically investigated, and the starting currents of the electron beam were found as functions of the parameters of a coaxial waveguide, constant magnetic field, beam injection energy, etc. In this paper, we consider a nonlinear regime of generation and investigate the operating modes of gyro-BWOs numerically for various values of the injection current of the electron beam.

## 2. Statement of the Problem. The Basic Equations

Let's consider the coaxial waveguide formed by two coaxial cylinders with length  $L$  and radii  $a$  and  $b$  ( $a > b$ ). At the input  $z = 0$ , the monoenergetic beam with an initial distribution function

$$f_0 = n_b \delta(p_\perp^2 - p_{\perp 0}^2) \delta(p_\parallel - p_{\parallel 0}) / \pi \quad (1)$$

is injected. Here,  $n_b$  is the electron beam density,  $p_{\perp 0}$  and  $p_{\parallel 0}$  are the initial transverse and longitudinal momenta, respectively. The injected beam has inner radius  $r_b$  and thickness  $\Delta b$ . The system is immersed into a longitudinal magnetic field  $H(z) = H_0 h(z)$ , where a function  $h(z)$  describes a slow change of the external magnetic field along the system length. The interaction of the electron beam with an eigenmode of the smooth waveguide takes place only under the resonance condition on the normal Doppler effect  $\omega - k_\parallel V_\parallel \simeq n\Omega_H/\gamma$ , where  $\omega$  is the frequency of an excited wave,  $k_\parallel$  is the longitudinal wave number of an excited wave,  $\Omega_H = |e|H_0/mc$ ,  $e$  is the charge of an electron,  $m$  is the mass of an electron,  $c$  is the velocity of light  $n=0, \pm 1, \pm 2, \dots$ ,  $V_\parallel = p_\parallel/m\gamma$  and  $\gamma$  are the longitudinal velocity and the relativistic factor of the electron beam, respectively.

In this paper, we consider the interaction of an electron beam, for which the condition of the Doppler resonance  $n = 1$  is satisfied, with a backward wave of the coaxial waveguide  $k_\parallel < 0$ .

For the description of the given interaction of an electron beam with a backward wave  $TE_{01}$  of the coaxial waveguide, we make use of the equations for nonzero components of the electromagnetic field  $E_\varphi$ ,  $H_r$ ,  $H_z$  and the equations of motion of beam particles in Lagrange variables.

While deriving the nonlinear equations for the amplitude  $E_\varphi$  of an eigenwave of the coaxial waveguide excited by an electron beam and the equations of motion of particles of the beam, we use the following assumptions: a slow changing of the amplitude  $\tilde{E}_\varphi$  of the HF-field over distances about a wavelength,

$$\left| \frac{1}{\tilde{E}_\varphi(z, t)} \frac{\partial \tilde{E}_\varphi}{\partial z} \right| \ll |k_\parallel|, \quad (2)$$

and a slow temporal changing of the HF-field amplitude,

$$\left| \frac{1}{\tilde{E}_\varphi(z, t)} \frac{\partial \tilde{E}_\varphi}{\partial t} \right| \ll \omega. \quad (3)$$

Supposing that the electron beam does not change the radial structure of the HF-field, we obtain the following

system of nonlinear equations:

$$\frac{\partial C_\varphi}{\partial \tau} - \frac{\partial C_\varphi}{\partial \xi} = \frac{i\alpha}{2\pi} \int_0^{2\pi} d\Psi(0) \times \int_{\rho_b}^{\rho_b + \Delta} \bar{\rho}(0) d\bar{\rho}(0) \frac{a_\perp}{a_\parallel} e^{i\Psi} \Phi_1(\bar{\rho}) J_1'(\bar{k}_\perp a_\perp / \omega_H), \quad (4)$$

$$\frac{d\bar{\rho}}{d\xi} = -\frac{1}{2} \frac{\bar{\rho}}{\omega_H} \frac{\partial \omega_H}{\partial \xi} + \frac{\gamma}{a_\parallel} + \left\{ -\frac{\bar{k}_\perp}{\omega_H} \left( 1 - \frac{\bar{k}_\parallel a_\parallel}{\gamma} - \frac{\omega_H}{\gamma} \right) \Phi_1(\bar{\rho}) J_1'(\bar{k}_\perp a_\perp / \omega_H) + \frac{\bar{k}_\perp^2 a_\perp}{\gamma \omega_H \bar{\rho} \Phi_1'(\bar{\rho}) J_1(\bar{k}_\perp a_\perp / \omega_H)} \right\} \frac{1}{2} (iC_\varphi e^{-i\Psi} + \text{c.c.}), \quad (5)$$

$$\frac{da_\perp}{d\xi} = \frac{1}{2} \frac{a_\perp}{\omega_H} \frac{\partial \omega_H}{\partial \xi} + \left( \frac{\gamma}{a_\parallel} - \bar{k}_\parallel \right) \times \Phi_1(\bar{\rho}) J_1'(\bar{k}_\perp a_\perp / \omega_H) \frac{1}{2} (iC_\varphi e^{-i\Psi} + \text{c.c.}), \quad (6)$$

$$\frac{d\gamma}{d\xi} = \frac{a_\perp}{a_\parallel} \Phi_1(\bar{\rho}) J_1'(\bar{k}_\perp a_\perp / \omega_H) \frac{1}{2} (iC_\varphi e^{-i\Psi} + \text{c.c.}), \quad (7)$$

$$\frac{da_\parallel}{d\xi} = -\frac{1}{2} \frac{a_\perp^2}{a_\parallel} \frac{1}{\omega_H} \frac{\partial \omega_H}{\partial \xi} + \frac{a_\perp \bar{k}_\parallel}{a_\parallel} \times \Phi_1(\bar{\rho}) J_1'(\bar{k}_\perp a_\perp / \omega_H) \frac{1}{2} [iC_\varphi e^{-i\Psi} + \text{c.c.}]. \quad (8)$$

$$\frac{d\Psi}{d\xi} = \frac{\gamma}{a_\parallel} - \bar{k}_\perp - \frac{\omega_H}{a_\parallel} + \frac{\bar{k}_\perp}{2a_\parallel} \left[ \left( -1 + \left( 1 - \frac{\bar{k}_\parallel a_\parallel}{\gamma} - \frac{\omega_H}{\gamma} \right) \times \frac{\gamma}{\omega_H} \left( \frac{\omega_H^2}{\bar{k}_\perp^2 a_\perp^2} - \frac{1}{\bar{\rho}^2} \right) + \frac{\omega_H^2}{\bar{k}_\perp^2 a_\perp^2} \right) J_1(\bar{k}_\perp a_\perp / \omega_H) + \frac{\bar{k}_\perp a_\perp}{\omega_H \bar{\rho}} J_1'(\bar{k}_\perp a_\perp / \omega_H) \right] \Phi_1(\bar{\rho}) (C_\varphi e^{-i\Psi} + \text{c.c.}). \quad (9)$$

Here, we have introduced the following dimensionless quantities:  $\rho_b = r_b k_\perp$ ,  $\bar{\rho} = \bar{r} k_\perp$ ,  $\Delta = k_\perp \Delta b$  is the normalized thickness of the beam,

$$\tau = -k_\parallel ct, \quad \xi = \frac{\omega}{c} z, \quad \omega_H = \frac{\Omega_H}{\omega}, \quad C_\varphi = \frac{|e| \tilde{E}_\varphi}{mc\omega},$$

$$a_\perp = \frac{p_\perp}{m_0 c}, \quad a_\parallel = \frac{p_\parallel}{m_0 c}, \quad \bar{k}_\parallel = \frac{k_\parallel c}{\omega},$$

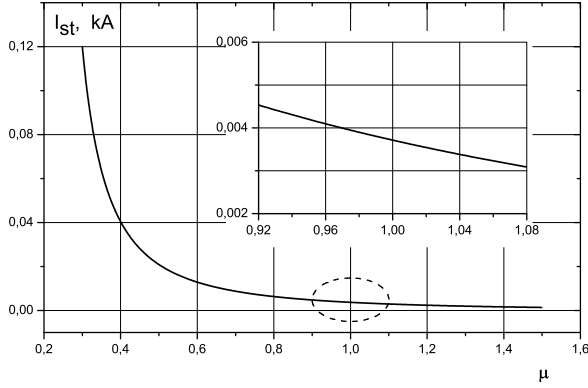


Fig. 1. Starting current  $I_{st}$  versus the ratio of the initial transversal momentum of a beam to the initial longitudinal one,  $\mu$ , for the coaxial waveguide length  $L = 60$  cm; the inner waveguide radius  $b = 3$  cm; outer waveguide radius  $a = 5$  cm; generation frequency  $f \approx 7.7$  GHz; inner beam radius is 3.9 cm; outer beam radius is 4.1 cm; beam energy is  $E = 511$  keV ( $\gamma_0 = 2$ )

$$\bar{k}_\perp = \frac{k_\perp c}{\omega}, \quad \gamma = \sqrt{1 + a_\perp^2 + a_\parallel^2},$$

$S_b = \pi(2r_b + \Delta b)\Delta b$  is a cross-section area of the beam,  $J_1(x)$  is the first-order Bessel function,  $J'_1(x) \equiv \frac{dJ_1(x)}{dx}$ ,  $\alpha = -\frac{2\pi}{S_b \|\Phi_1\|^2 k_\perp^2 k_\parallel} \frac{c^4 I_b}{\omega^4 I_A}$ ,  $I_b$  is the beam current,  $I_A = \frac{mc^3}{e} = 17.06$  kA, and  $\|\Phi_1\|^2 = \int_b^a \Phi_1^2(k_\perp r) r dr$ . The function  $\Phi_1(k_\perp r)$  describes the radial structure of the wave field,<sup>4</sup>

$$\Phi_1(k_\perp r) = J_1(k_\perp r) - \frac{J_1(k_\perp a)}{N_1(k_\perp a)} N_1(k_\perp r), \quad (10)$$

and  $N_1(x)$  is the first-order Neumann function. The function  $\Psi = \omega t_L - k_\parallel z - \theta + \bar{\varphi}$  describes the phase of a particle relative to the wave,  $t_L$  is the arrival time of a particle at the point with the coordinate  $z$  (Lagrange time),  $\theta$  is an angle in the momentum space  $\text{tg } \theta = p_x/p_y$ , and  $p_\perp = (p_x^2 + p_y^2)^{1/2}$ .

The transversal wavenumber  $k_\perp$  is determined by solving the dispersion equation

$$\Phi_1(k_\perp b) = 0. \quad (11)$$

By deducing the system of equations (4), we have used the Liouville theorem on the conservation of a phase volume along the trajectories of movement of particles:

$$f d^3 p d^3 r = f_0 d^3 p(0) d^3 r(0).$$

Here,  $f_0$  is the initial distribution function,  $d^3 p(0) d^3 r(0)$  is the phase volume of particles of the beam in the injection plane  $z = 0$ . We have substituted the variables  $r$  and  $\varphi$  ( $r$  is the radius of a trajectory of particles of the beam,  $\text{tg } \varphi = y/x$ ,  $y$  is the projection of the radius-vector of a particle onto the  $OY$  axis, and  $x$  is the projection of the radius-vector of a particle onto the  $OX$  axis) by the variables  $\bar{r}$  and  $\bar{\varphi}$  ( $\bar{r}$  is the radius of the driving center of a Larmor orbit of electrons, and  $\bar{\varphi}$  is the azimuthal angle of a Larmor orbit) according to the formulas

$$r^2 = \bar{r}^2 + \frac{p_\perp^2}{m^2 \Omega_H^2} + \frac{2p_\perp \bar{r}}{m \Omega_H} \sin(\theta - \bar{\varphi}),$$

$$\varphi = \bar{\varphi} - \frac{p_\perp}{m \Omega_H \bar{r}} \cos(\theta - \bar{\varphi}).$$

Let's add Eqs. (4)–(9) by the boundary conditions for the amplitude of an excited wave and for particles of the beam:

$$\Psi|_{\xi=0} \in [-\pi, \pi], \quad \gamma|_{\xi=0} = \gamma_0,$$

$$(a_\perp/a_\parallel)|_{\xi=0} = \mu, \quad C_\varphi|_{\xi=\bar{L}} = 0, \quad C_\varphi|_{\xi=0} = C_{\varphi 0}. \quad (12)$$

Here,  $\bar{L} = \omega L/c$  is the dimensionless length of the system.

By linearizing the system of equations (4)–(9) and taking into account the boundary conditions (12), we get a transcendental equation and use numerical methods to determine the dependence of a starting current  $I_{st}$  on parameters of the system (the installation length  $L$ , the beam energy  $\gamma$ , etc.). In more details, the results of investigations of these dependences are presented in [3]. It is necessary to recall that the starting current decreases rapidly with increase in the ratio of the initial transversal momentum to the longitudinal one,  $\mu$ . Moreover, the present nonlinear analysis has shown that the interaction efficiency also depends strongly on the parameter  $\mu$ . A high (by the criteria concerning the operation of gyro-BWOs) efficiency can be achieved for relatively large values  $\mu$ . But, the starting currents in this case are not given in the cited work [3].

In Fig. 1, we show the dependence  $I_{st}(\mu)$  derived for a homogeneous magnetic field  $h(z) = 1$  with the following parameters: the oscillation frequency  $f_0 = 7.7$  GHz, inner radius of the coaxial waveguide of a gyro-BWO  $b = 3$  cm, outer radius  $a = 5$  cm, inner beam radius  $r_b = 3.9$  cm, outer beam radius  $r_a = 4.1$  cm, energy of the injected electron beam  $E = 511$  keV ( $\gamma_0 = 2$ ), and system length  $L = 60$  cm. As follows from this plot, the starting current strongly increases with decrease in the ratio of the initial

transversal momentum to the longitudinal one. At  $\mu = 1$ , the starting current  $I_{st} = 3.7$  A. We note that, for the given beam energy and the geometric sizes of a generator, the limiting vacuum current  $I_{lim} = 6.6$  kA [4].

The investigation of nonlinear regimes was carried out for numerical values of the parameters mentioned above and also for  $\mu = 1$ . The value of the initial amplitude was chosen to be equal to  $C_{\varphi 0} = 5 \cdot 10^{-4}$ . The control over the accuracy of calculations was performed with the help of the conservation law

$$\frac{\partial}{\partial \tau} \left[ \int_0^{\bar{L}} d\xi |C_{\varphi}(\xi, \tau)|^2 \right] + |C_{\varphi}(\xi = 0, \tau)|^2 + \frac{\alpha}{\pi} \int_{\rho_b}^{\rho_b + \Delta} d\rho(0) \int_0^{2\pi} d\Psi(0) \bar{\rho}(0) [\gamma(\xi = \bar{L}, \tau) - \gamma_0] = 0. \quad (13)$$

The precision of the fulfillment of the conservation law in our calculations at the fixed values of temporal and spatial steps depended on the current of an electron beam. At low and middle values of the beam current (up to 1 kA), the accuracy was not worse than fractions of one percent. At the currents close to the limiting vacuum current, the accuracy becomes worse but was, in any case, at most several percents.

Starting from a conservation law, it is possible to determine the interaction efficiency as

$$\eta(\tau) = \frac{\int_{\rho_b}^{\rho_b + \Delta} d\rho(0) \int_0^{2\pi} d\Psi(0) \bar{\rho}(0) [\gamma(\xi = L, \tau) - \gamma_0]}{\pi [(\rho_b + \Delta)^2 - \rho_b^2] (1 - \gamma_0)}. \quad (14)$$

The results of the nonlinear analysis which has been carried out for various beam currents consist in the following. If the beam current  $I$  is less than 4 A, the system is not excited. Such beam current well coincides with the starting current  $I_{st} = 3.7$  A derived in the linear approximation (see Fig. 1). The self-excitation of oscillations occurs at  $I > I_{st}$ . A small excess of the injected beam current above the starting current leads to the steady-state generation regime. In Fig. 2, *a* the temporal variation of the backward wave amplitude at the system input is given for  $I = 4$  A. It follows from this plot that, at the initial stage, the amplitude grows exponentially, and the steady-state operation regime takes place after some oscillations beginning from  $\tau = 1000$ . The investigation of the spatial distribution of the amplitude in the stationary mode of generation (Fig. 3) shows the following. The distribution of the field amplitude along the system length at a fixed moment of

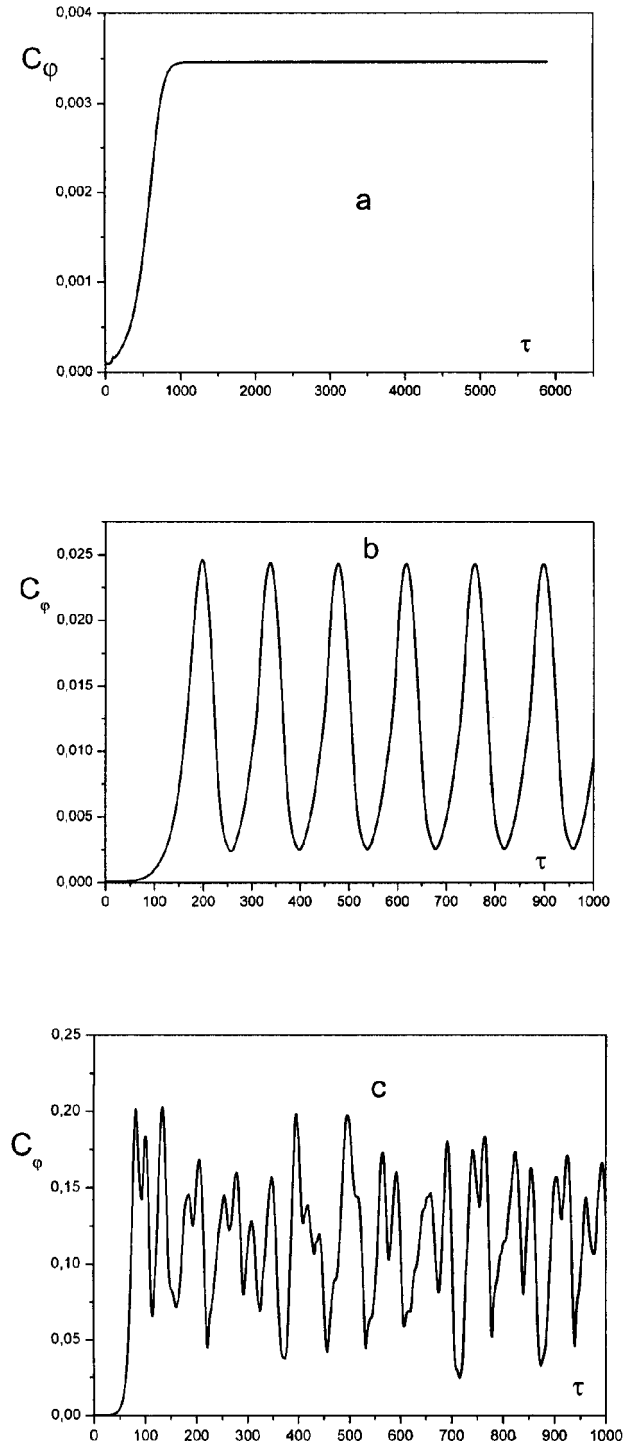


Fig. 2. Normalized amplitude of an excited wave vs the dimensionless time: *a* —  $I = 4$  A, *b* —  $I = 15$  A, *c* —  $I = 0.6$  kA. The ratio of the initial transversal momentum of a beam to the initial longitudinal one  $\mu = 1$ . The rest of parameters are the same as in Fig. 1

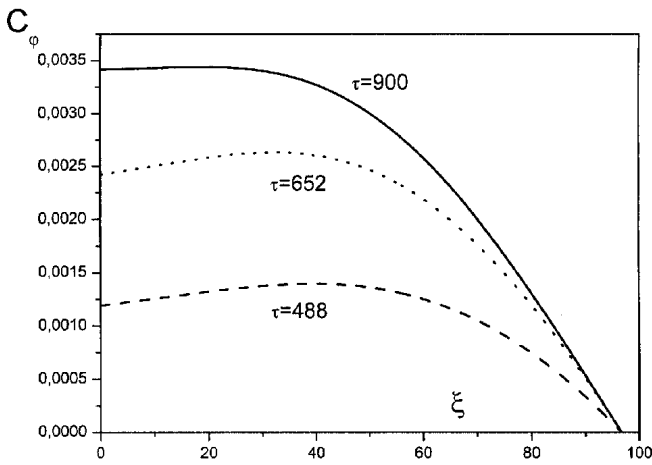


Fig. 3. Axial distribution of the normalized amplitude of an excited wave for the steady-state regime ( $I = 4$  A, see Fig. 2, *a*) in different time moments: the dashed line corresponds to  $\tau = 488$ , dotted line corresponds to  $\tau = 652$ , and solid line corresponds to  $\tau = 900$ . The rest of parameters are the same as in Fig. 2

time is the curve with one maximum which originates closely to  $\xi = \bar{L}$  and then is displaced to the injection plane with a velocity close to the group velocity. Beginning from  $\tau \geq 1000$ , the invariable field distribution is established along all the interaction region with a maximum near the input face.

For higher beam current values,  $I \geq 15$  A, the steady-state regime of oscillation becomes unstable, and the self-modulation regime of oscillation is established. The typical temporal dynamics of the field amplitude is given in Fig. 2, *b* ( $I = 15$  A). In this case, the period of self-modulation oscillations is approximately equal to the transit time of a signal through a feedback circuit  $T_m = L/|V_{||}(0) + L/|V_g|$ . The spatial distribution of the self-modulation field has a complex character with several maxima (Fig. 4) along the system length. The self-modulation regime of operation is observed up to current values  $I < 60$  A. At the further increase in the beam current, such a mode of oscillation is changed into the stochastic regime of operation (see Fig. 2, *c*).

To determine the frequency characteristics of a output signal, we performed the spectrum analysis by the following formulas:

$$S(f) = \lg \frac{|P(f)|^2}{|P_{\max}(f)|^2},$$

$$P(f) = \frac{1}{T} \int_0^T \frac{1}{2} (C_\varphi(\xi = 0, t) e^{-i2\pi f_0 t} + \text{c.c.}) e^{i2\pi f t} dt. \quad (15)$$

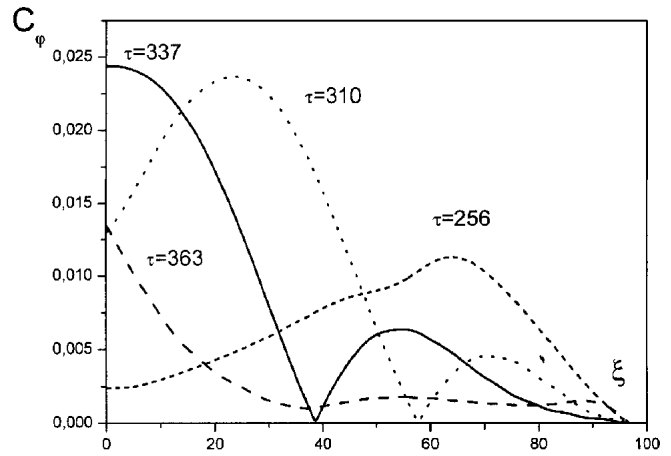


Fig. 4. Axial distribution of the normalized amplitude of an excited wave for the periodic self-modulation regime ( $I = 15$  A, see Fig. 2, *b*) in different time moments: the short dashed line corresponds to  $\tau = 256$ , dotted line corresponds to  $\tau = 310$ , solid line corresponds to  $\tau = 337$ , and long dashed line corresponds to  $\tau = 363$ . The rest of parameters are the same as in Fig. 2

Here,  $P_{\max}$  is the maximal value of  $P(f)$ , and  $T$  is the duration of a temporal realization.

In Fig. 5, *a* the output signal spectrum corresponding to the steady-state operation regime ( $I = 4$  A) is shown. The one-frequency mode with the frequency close to  $f \approx 7.7$  GHz is realized for the steady-state regime. With increase in the current, the oscillation frequency corresponding to the power peak is displaced to higher frequencies, and a number of equidistant peaks appears. For example, at a current  $I = 15$  A, the maximum of spectral power is located at  $f \approx 7.73$  GHz, and the equidistant peaks are tuned one from another by  $\Delta f \approx 60$  MHz (see Fig. 5, *b*). The spectral power harmonics nearest to the maximum have the values comparable to the spectral power at the fundamental frequency. Upon the further increase in the beam current, the number of equidistant maxima grows, and each of them is widened. Finally, the spectrum becomes continuous. The typical diagram of the spectral density is given on Fig. 5, *c* for the beam current  $I = 0.6$  kA. We note that the dynamics of changing the generation regimes in the coaxial structure and the behavior of the spectral density under variation of the injected current qualitatively are in close agreement with an analogous behavior of a cylindrical gyro-BWO [5].

The efficiency of HF oscillations determined according to (14) oscillates in time in the self-modulation and stochastic modes with a great modulation depth. Therefore, to describe the oscillation efficiency, it makes

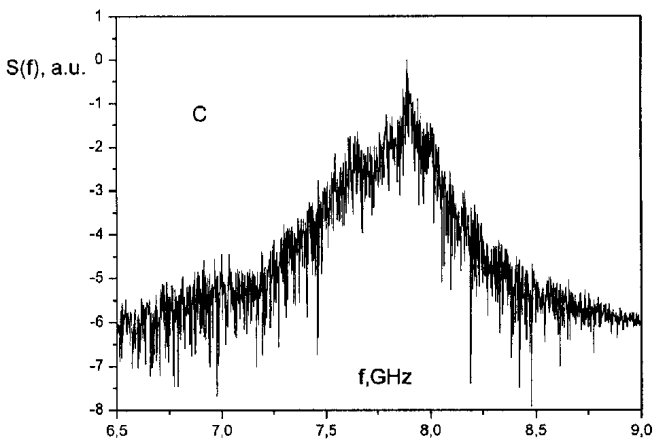
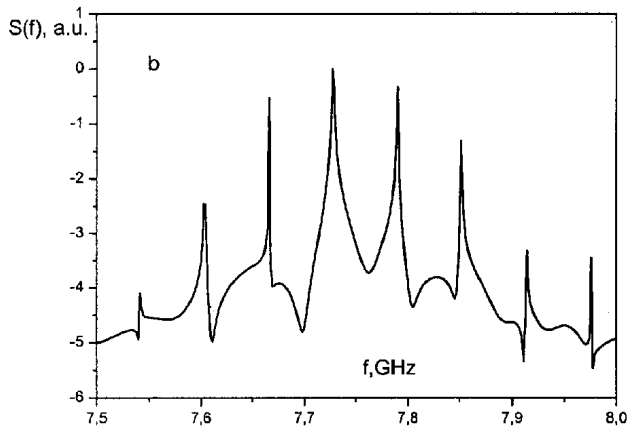
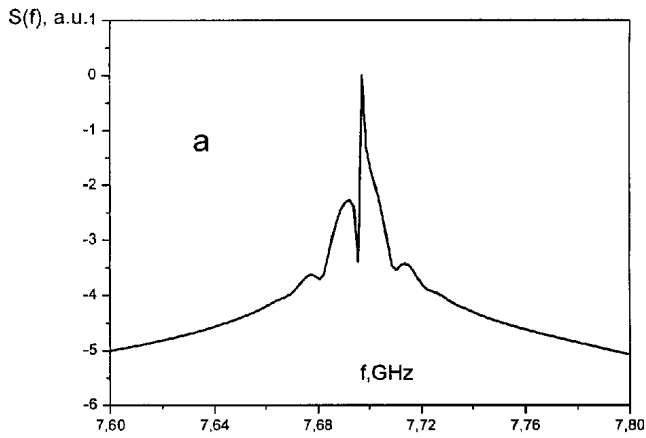


Fig. 5. Spectrum density of an excited wave versus the frequency: *a* –  $I = 4$  A, *b* –  $I = 15$  A, *c* –  $I = 0.6$  kA. The rest of parameters are the same as in Fig. 2

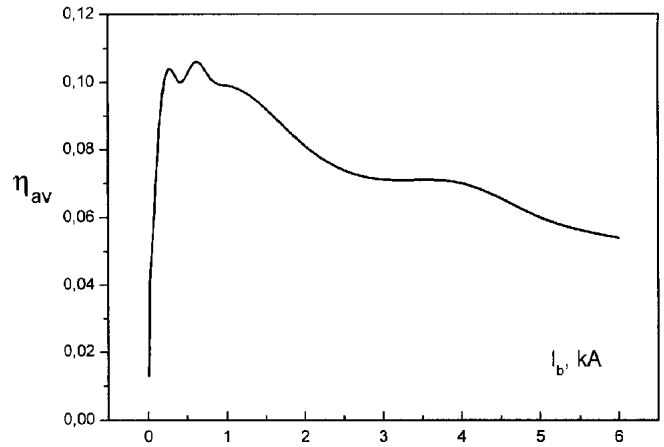


Fig. 6. Beam interaction efficiency in a coaxial gyro-BWO versus the beam current. The rest of parameters are the same as in Fig. 2

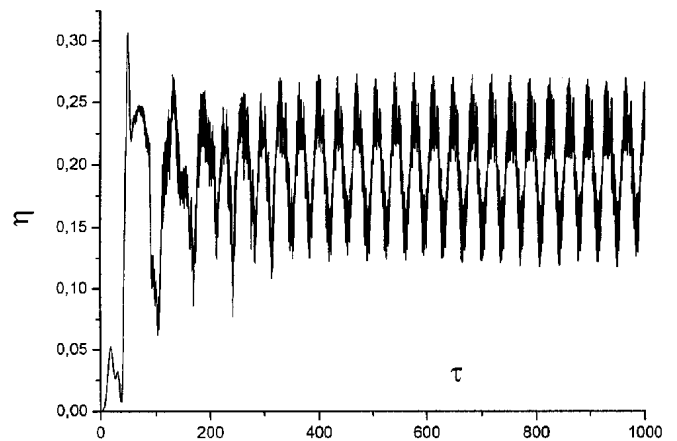


Fig. 7. Beam interaction efficiency in a coaxial gyro-BWO versus the dimensionless time in the case of an inhomogeneous magnetic field (16). The inhomogeneity gradient  $\lambda = 0.3$ . The rest of parameters are the same as in Fig. 2

sense to carry out the temporal averaging of the efficiency. In Fig. 6, the dependence of the average efficiency  $\bar{\eta}$  on the beam current is presented. The efficiency of oscillation is low near the threshold of HF field generation. At the current  $I = 4$  A corresponding to the steady-state regime,  $\bar{\eta} = 1.2\%$ . The efficiency is higher in the self-modulation regime, but it is still low enough. For a current  $I = 15$  A, the efficiency  $\bar{\eta} = 3.5\%$ . The greatest efficiency is obtained in the stochastic regime. The maximum of efficiency,  $\bar{\eta} = 10.6\%$ , is reached at the beam current  $I = 0.6$  kA. At the further increase in the beam current, the oscillation efficiency slowly decreases.

The results of calculations confirm that the essential drawback of the considered devices, as was noted in

the introduction, is the small efficiency. One of the possibilities to increase the efficiency is to use a tapered magnetic field varying along the interaction gap. In the simple case, it is possible to change the magnetic field by a linear law [2]

$$h(\xi) = 1 + \lambda\xi/\bar{L}. \quad (16)$$

In Fig. 7, we show the temporal dynamics of the interaction efficiency (14) obtained as a result of the numerical solution of the system of equations (4)–(9) for the inhomogeneity gradient  $\lambda = 0.3$  and the beam current  $I = 0.6$  kA. As compared to the case of a homogeneous magnetic field, the efficiency has increased up to 20 %, i.e. almost twice. We note that a small inhomogeneity of the magnetic field changes not only the oscillation efficiency but also the spectral characteristics of the oscillation regime. For example, the self-modulation regime, when setting an inhomogeneity of the magnetic field, can pass to the steady-state oscillation regime. We are going to give a detailed investigation of the operation of a coaxial gyro-BWO in the applied tapered magnetic field elsewhere.

### 3. Conclusions

On the basis of the numerical solution of the system of nonlinear equations, we have studied the mechanisms of the transition to a stochastic regime of oscillation in a coaxial gyro-BWO. It is shown that, with increase in the current of an injected electron beam, the steady-state operation regime changes into a self-modulation regime

which becomes further more complicated and stochastic. The numerical results have shown that applying a tapered magnetic field for the given type of devices leads to a considerable increase in the efficiency.

1. *Ginzburg N.S., Zarnitsyna N.G., Nusinovich G.S.* // Radiotekh. Elektr. — 1979. — **24**, N6. — P.1146–1152.
2. *Ganguly A.K., Ahn S.* // Intern. J. Electronics. — 1989. — **67**, N2. — P.261–276.
3. *Borodkin A., Khoruzhiy V., Onishchenko I., Sotnikov G.* // Ukr. J. Phys. — 2004. — **49**, N2. — P.126–131.
4. *Sotnikov G.V., Yatsenko T.Yu.* // Techn. Phys. — 2002. — **47**, N5. — P.535–538.
5. *Ginzburg N.S., Zaitsev N.I., Ilyakov E.V. et.al.* // Proc. 5th Intern. Workshop “Strong Microwaves in Plasmas”, Nizhny Novgorod, 2003. — Vol.1. — P.144–150.

Received 27.12.04

### КОАКСІАЛЬНА ГИРО-ЛЗХ. 2. НЕЛІНІЙНА ТЕОРІЯ

*А.В. Бородкін, І.Н. Оніщенко, Г.В. Сотніков,  
В.М. Хоружий*

#### Резюме

Проведено теоретичні і чисельні дослідження нелінійного режиму генерації в коаксіальній лампі на зворотній хвилі (гіро-ЛЗХ), що використовує резонанс електронного пучка з власною хвилею гіро-ЛЗХ на нормальному ефекті Доплера. Аналізуються часові і просторові залежності амплітуди напруженості ВЧ-хвилі в коаксіальному хвилеводі для різних значень струмів інжекції електронного пучка. Досліджено типи режимів збудження коаксіальної гіро-ЛЗХ і поведінку ефективності взаємодії зі зміною струму електронного пучка.